An Optimal Algorithm for Resource Optimization in 5G Networks Based on Machine Learning

*Dong Sang, Hongwei Sun**

Department of Computer Science and Engineering, Weifang University, China
sangdongd@126.com, hongwei.sun163@gmail.com

Abstract

A 5G network enabling technology to meet multi-gabit data demands is mmwave D2D communications. As a result of their directional coverage and high data rate connectivity, mmwave networks are well suited for the delivery of proximity services via D2D communications. In a dense D2D pair network situation, the directional features at the mmwave band reduce interference between D2D pairs. To evaluate the impact of the integration of D2D and mmWave communication, this paper proposed a novel algorithm. The main idea is to maximize the total system throughput through optimal objective function. The linear correlation method is used to select the admission set of D2D users. Then, the optimal transmit power is determined through a power control mechanism. Finally, the resources are allocated to the D2D users using a multi-phase matching algorithm. Simulation results show that the proposed algorithm has better performance as compared with existing algorithms.

Keywords: Machine learning, Optimization, 5G network, Spectrum utilization

1 Introduction

The need for increased data rates and call traffic density per cell is increasing substantially along with the number of data-intensive applications [1]. Due to limited bandwidth, existing 4G technology is unable to keep up with the rising demand. The millimeter wave (mmWave) spectrum will be investigated as part of the development of 5G cellular technology [2]. Reducing interference can enhance the transmission quality of mmWave because of its high frequency and short-distance attenuation properties. At 28 GHz and higher, the outdoor propagation environment offers abundant multipath that may be leveraged to increase the received signal strength, particularly in the event of non-line-of-sight (NLOS) propagation [3]. Additionally, directional beamforming and smart antennas can enhance the quality of a link's propagation [4].

Device-to-device (D2D) technology enables direct communication between base station-controlled devices without the requirement for base station forwarding [5]. D2D technology allows for the connection of two devices, a reduction in base station load, and increased user concurrency. Great data rates and high spectrum efficiency are two benefits, but they also boost throughput and cut down on delays [6]. Applying D2D communication technology to cellular networks, utilizing the short-distance communication properties and direct communication methods of D2D technology itself, fully exploits the enormous benefits and potentials of D2D in terms of saving wireless resources, reducing system interference, and providing services, network coverage, improving wireless resource utilization efficiency and system capacity, and better adapting to user needs [7].

To cohabit with conventional cellular connectivity, adjacent devices can interact with one another through extra signaling and control [8].

High bandwidth and spectrum efficiency are benefits that a 5G network would experience when mmWave technology and D2D communication are used [9]. Additionally, D2D is based on proximity connection, whereas mmWave is a short-distance communication, making it easier to combine the benefits of the two technologies. It can be found either concentrated or scattered at the border of a cell or in a crowded area [10]. Inter-D2D interference during numerous D2D connections and interference between D2D and base station-to-device communication both occur in such a network. Therefore, in concurrent D2D and mmWave networks, efficient resource-sharing and interference avoidance strategies must be used. A resource allocation approach with the highest weighted matching ratio fairness is used in [11]. Utilize the maximum weighted matching method to distribute available resources for D2D users to optimize the system's overall weighted sum rate after first adjusting the power of the user to maximize the user's weighted sum rate. However, when a certain need is satisfied, a random selection is made for the multiplexing pair that consists of the cellular user and the D2D user. Therefore, even if the system performance has somewhat improved, more study is still required. In [12], the wireless resource allocation problem was transformed into a mixed integer nonlinear programming problem, and a novel greedy heuristic algorithm was proposed. This algorithm makes use of channel gain information to lessen interference with the cellular network, increasing the cell's overall throughput. By optimizing the overall rate allocation technique while fulfilling the signal-to-interference-plus-noise ratio (SINR) of cellular users

*Corresponding Author: Hongwei Sun; E-mail: hongwei.sun163@gmail.com
DOI: https://doi.org/10.70003/160792642024122507006

and D2D users, Reference [13] distributes resources for D2D users. The authors in [14-15] may provide quality of service (QoS) guarantees on a specific basis, but there is only so much that can be done to increase system throughput. MmWave D2D transmission takes place primarily indoors and less frequently outside. Directional uplink measurements for mmWave propagation in 5G networks are covered in [16]. An efficient method for downloading well-liked information in millimeter-wave tiny cells is suggested in [17]. This network's short-range and parallel D2D communication transmission increases transmission efficiency. The 28 GHz band is preferable to other mmWave bands because there isn't much research on mmWave bands in outdoor settings, and references [18-19] state as much. To increase the overall system throughput, the D2D resource allocation problem in the outdoor urban cellular network operating at 28 GHz is primarily investigated.

The authors in [20] proposes a resource allocation scheme, but this scheme only considers the interference caused by a single D2D user and ignores the overall interference caused by all D2D users to the system. Reference [21] studies an energy efficiency algorithm that uses Lagrangian duality theory and jointly optimizes power and data rate to increase the energy efficiency of D2D networks. However, this algorithm does not consider the overall interference caused by D2D communication to cellular communication. The authors in [22] proposed a spectrum resource management scheme under the 28 GHz bandwidth, which improved the system throughput to a certain extent, but it only simply allocated resources to D2D users. The resource-sharing scheme in [23] allows interference-free D2D links to share resources and maintains good network connectivity while improving network capacity. However, interference is inevitable in practical applications.

The authors in [24] proposed that high-frequency microwave backhaul is a feasible solution for ultra-dense small cell backhaul links in non-line-of-sight (NLOS) environments. Based on simulation and measurement results, it was concluded that the wireless backhaul solution is suitable for ultra-dense networks. Make the right choice. On this basis, reference [25] analyzed the impact of different frequency bands on the energy efficiency of the backhaul network in two typical UDN backhaul scenarios, showing that distributed solutions have more advantages than centralized solutions and are suitable for future 5G networks. environment. However, many solutions require a macro base station (MBS) or a specific (SBS) to forward data from the source to the destination. This solution has a large path loss during the transmission process, which can easily lead to an increase in the bit error rate. Moreover, when two users are close to each other, they can communicate directly through short-range communication technologies such as Bluetooth. When two users are far apart, they cannot communicate directly. Communication is possible using device-to-device (D2D) communication capabilities, which allow two nearby devices to communicate with each other within the licensed cellular bandwidth without a base station (BS) involved or limited by the BS. This is a dramatic departure from traditional cellular architecture [26].

In light of this, this paper proposed a novel approach for 5G network-based machine learning. The main contributions are as follows.

- A multi-stage bipartite graph-based matching method that can choose the best D2D user-sharing resources for mobile users.
- The set of cellular users that can be reused by each D2D user is determined using the linear correlation approach before resource allocation, under the condition that the QoS of cellular users and D2D users is satisfied.
- The D2D users manage power at the same time to maximize their throughput. Additionally, the mmWave frequency band has more resource blocks available than the LTE-Advanced system, which more than fulfills the technical requirements of communication standards in 5G application scenarios.

2 System Model and Problem Formulation

2.1 System Model

Assuming that the uplink resources in the cellular system are utilized to discuss the underlay approach in the 28 GHz cellular network in the 5G urban cellular network scenario where D2D users and cellular users coexist [27-28]. a distribution strategy that allows numerous D2D user pairs to share the same resource.

The interference between D2D users and cellular user equipment (CUEs) in this situation cannot be avoided, and it also cannot be disregarded when numerous D2D users are utilizing the same resources [29]. Assuming that each cellular user is given a mutually orthogonal resource block (RB), the set $C = \{1, 2, 3, \ldots, N\}$ stores the number of RBs, while the set $D = \{d = 1, 2, 3, \ldots, M\}$ contains the amounts for D2D pairs. Figure 1 displays a schematic of the interference produced when $D2D_1$ and $D2D_3$ multiplex the same cellular user CUE_1 [30].

2.2 Transfer Model

The authors in [31] gathered extensive measurement data while taking into account the real outdoor 28 GHz mmWave transmission circumstances and produced an intricate channel spatial statistical model. Under such dense user and obstacle settings, when angular signals are repeated with various delays, line-of-sight (LOS) transmission is impracticable.

As a result, in this case, the received signal suffers from both line-of-sight (LOS) and non-line-of-sight (NLOS) route losses, along with the accompanying shadow fading of each portion [32-33]. The route loss model is therefore calculated as $PL = PL_{LOS} + PL_{NLOS}$. The distance model predicts the following given the distance d:

$$PL_X(d) = \mu + 10\alpha \log(d(m)) + \varepsilon \quad \textbf{(1)}$$

where ε is the response lognormal shading, which obeys $N(0, \sigma^2)$, α is the path loss exponent and μ is the path loss coefficient.

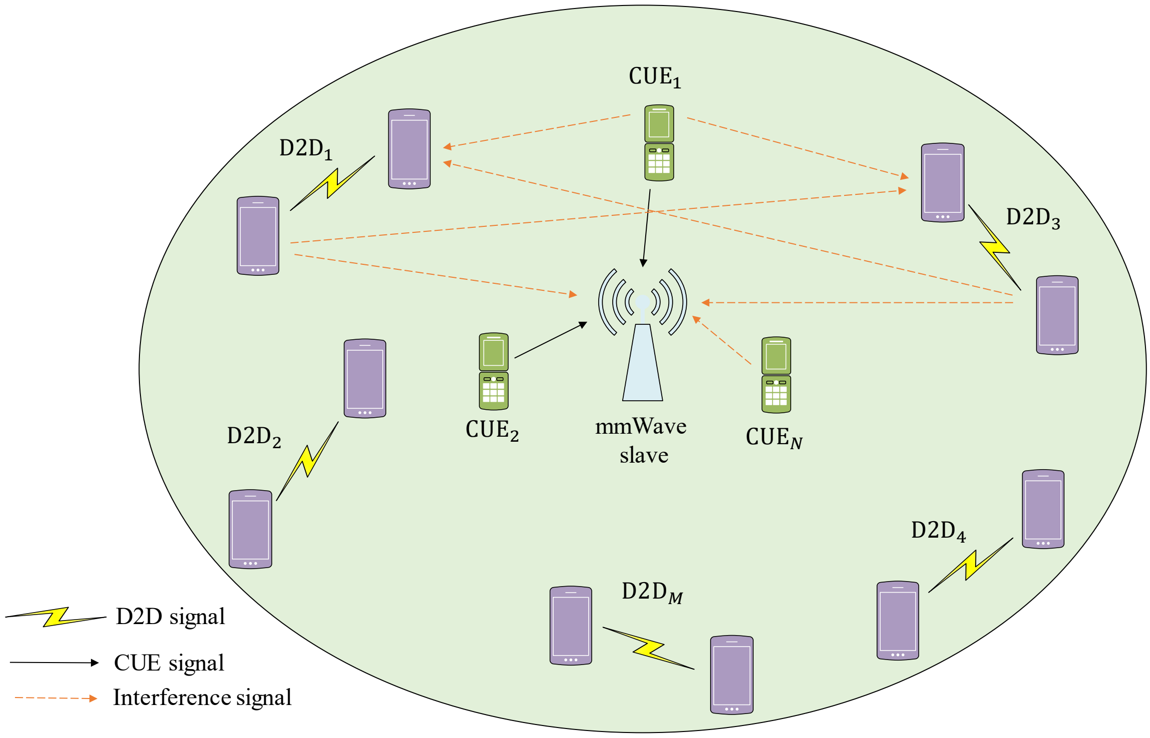

Figure 1. Schematic diagram of the interference generated when the same single-cell user CUE$_1$ is reused

In this case, the shadowing and lognormal path loss models are updated with the probabilities [34]. D2D lines typically receive more LoS signals because of the short-distance nature of D2D transmission.

Therefore, the path loss PL$_1$ of the D2D link is:

$$PL_1 = p_1 PL_{LOS} + (1 - p_1) PL_{NLOS} \tag{2}$$

The path loss PL$_2$ of other links is:

$$PL_2 = p_2 PL_{LOS} + (1 - p_2) PL_{NLOS} \tag{3}$$

The multipath fading in mmWave communications is the Rician channel.

2.3 Problem Description

The RBs of N N cellular users are allotted to M D2D users in a 28 GHz mmWave small cell network [35], and the allocation matrix $X = \{x_{c,d}\}_{N\times M}$ is utilized to describe the allocation outcome of the cellular user RBs. The primary objective of resource sharing is to increase overall throughput for both D2D and cellular users while maintaining both groups' SINRs [36]. The SINR r_c, r_d of cellular users and D2D users in this study is:

$$r_c = \frac{p_c H_{c,B}}{\Sigma_{d=1}^{M} x_{c,d} p_d H_{d,B} + N_c} \geq r_c^{th}, c = 1, 2, ..., N \tag{4}$$

$$r_d = \frac{p_d H_{d,d}}{\Sigma_{c=1}^{N} x_{c,d} p_c H_{c,d} + \Sigma_{c=1}^{N} \Sigma_{d' \in D\setminus\{d\}}^{M} x_{c,d'} p_{d'} H_{d',d} + N_d} \geq r_c^{th}, c = 1, 2, ..., N, d = 1, 2, ...M \tag{5}$$

Among them, p_c and p_d are the transmitting power of the cellular user and the D2D transmitter respectively; $H_{i,j}$ is the channel gain of the link i, j, N_c and N_d are Gaussian white noise, both are N_0 ; r_c^{th} , r_d^{th} are the SINR threshold of cellular and of D2D users; $x_{c,d}$ are binary variables [37-38], indicating whether the d-th D2D pair reuses the c-th cellular user resources, $x_{c,d} = 1$ means multiplexing; $x_{c,d} = 0$ means no multiplexing.

Where p_c and p_d are the transmitting power of the cellular user and the D2D transmitter, respectively; $H_{i,j}$ is the channel gain of the link i, j; N_c and N_d are AWGN [39], both of which are N_0 ; r_c^{th} ; r_d^{th} are the SINR thresholds of the cellular and the D2D users; and $x_{c,d}$ are binary variables that indicate whether the d-th D2D pair reuses the c-th cellular user resources, $x_{c,d}$ = 1 means multiplexing; $x_{c,d} = 0$ means no multiplexing [40].

From Shannon's formula, we get:

$$R_c = B \log(1 + r_c) \tag{6}$$

$$R_d = B \log(1 + r_d) \tag{7}$$

The maximizing problem may be phrased as follows if B is the bandwidth of the cellular user channel resources:

$$R = \max_{x} \left\{ \sum_{c=1}^{N} R_c + \sum_{d=1}^{M} R_d \right\}$$
$$= \max_{x} \left\{ \sum_{c=1}^{N} B \log(1 + \frac{p_c H_{c,B}}{\sum_{d=1}^{M} x_{c,d} p_d H_{d,B} + N_0} \right\}$$
$$+ \sum_{d=1}^{M} \left(1 + \frac{p_d H_{d,d}}{\sum_{c=1}^{N} x_{c,d} p_c H_{c,d} + \sum_{c=1}^{N} \sum_{d' \in D \backslash \{d\}}^{M} x_{c,d'} p_{d'} H_{d',d} + N_0} \right) \quad \textbf{(8)}$$

s.t.

$$\frac{p_c H_{c,B}}{\sum_{d=1}^{M} x_{c,d} p_d H_{d,B} + N_0} \geq r_c^{th}, c = 1,2,...,N \quad \textbf{(8a)}$$

$$d = 1,2,...,M \quad \textbf{(8b)}$$

$$p_c \leq p_c^{\max}, c = 1,2,...,N \quad \textbf{(8c)}$$

$$p_d \leq p_d^{\max}, d = 1,2,...,M \quad \textbf{(8d)}$$

$$\sum_{c \in C} x_{c,d} \leq 1, \forall d \in D \quad \textbf{(8e)}$$

Their respective maximum transmission powers for cellular and D2D users are $p_c^{\max}$ and $p_d^{\max}$. The constraint conditions to satisfy the SINR needs of cellular users and D2D users are represented by equations (8a) and (8b) [41-42]. Equations (8c) and (8d) represent the transmit power cap for cellular users and D2D users, respectively. A D2D user can only share resources with one cellular user, according to Eq. (8e).

The resource allocation strategy directly influences the system's throughput since the optimization objective is a difficult-to-attain nonlinear integer programming problem [43], especially when there are many D2D pairings. As a result, the following resource allocation strategy is used as a solution to this issue. First, the group of cellular users that may be utilized again by D2D users is identified using the linear correlation approach [44]. Next, apply power control to D2D users. To allocate spectrum resources across various users, a bipartite graph D2D resource allocation technique based on multi-stage matching is implemented [45-46].

3 Resource Allocation

3.1 D2D Reusable Cellular User Set

Using the linear programming approach, find the set of reusable cellular users for each D2D user to fulfill the requirement of satisfying the quality of service (QoS) for cellular users and D2D users [47-48].

As seen in Figure 2, the admission set of D2D users, which is the set of prospective multiplexed cellular users, is screened out using the linear programming approach to assure the QoS of cellular users and D2D users [49-50]. Each cellular user and each D2D user must adhere to formulas (8a) and (8b) if the cellular user c is a member of the set "_d," which may be written as follows:

$$b1: p_c H_{c,B} \geq r_c^{th}(p_d H_{d,B} + N_0)$$
$$b2: p_d H_{d,d} \geq r_d^{th}(p_c H_{c,B} + N_0) \quad \textbf{(9)}$$

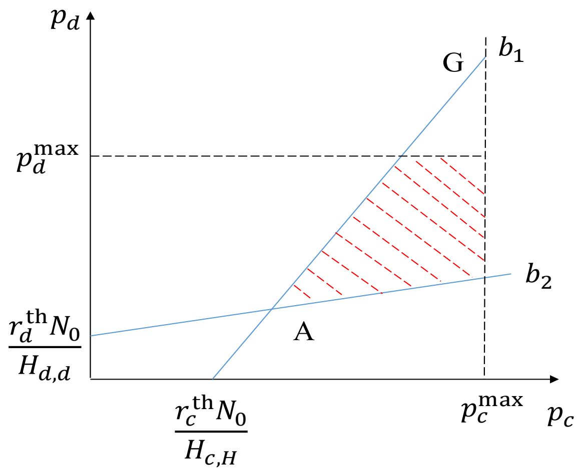

Figure 2. Selection of potential reuse objects

From the two inequalities in formula (9), the values of points A and G in Figure 2 can be obtained [51]:

$$A = \{x_A, y_A\}$$
$$= \left\{ \begin{array}{c} N_0 \dfrac{H_{d,d} r_c^{th} + H_{d,B} r_c^{th} r_d^{th}}{H_{d,d} H_{c,B} - r_c^{th} r_d^{th} H_{c,d} H_{c,B}} \\ \dfrac{H_{c,d} r_c^{th} r_d^{th} + H_{c,B} r_d^{th}}{H_{d,d} H_{c,B} - r_c^{th} r_d^{th} H_{c,d} H_{c,B}} \end{array} \right\} \quad \textbf{(10)}$$
$$G = (x_G, y_G) = \left\{ \begin{array}{c} p_c^{\max} \\ \dfrac{p_c^{\max} H_{j,B} - r_c^{th} N}{r_c^{th} H_{i,B}} \end{array} \right\}$$

In Figure 2, the D2D user only has a cellular user that shares resources with it when there is an intersecting point A [52-53]. Furthermore, the QoS of cellular users and D2D users can only be ensured when the intersection point A is in the region defined by the coordinate axis and the dotted line in Figure 2. The viable transmission power region of p_c and p_d is indicated in Figure 2 by the shaded area [54-55].

The channel gain of the D2D user and the cellular user must match the following formula (11) if the cellular user c is in the set Π_d,

$$\{x_A, y_A\} \leq \left(p_c^{\max}, p_d^{\max}\right) \quad \textbf{(11)}$$

Equation (11) is used to demonstrate that no end user's viable transmission power is higher than the maximum value.

3.2 Power Control for D2D Users

Power allocation is done on the D2D users if a cellular user $c \in \Pi_d$ and a D2D user share a cellular resource. The QoS needs of cellular users are met while D2D user throughput is increased [56]. Therefore, it is necessary to suitably limit the transmit power of cellular users while raising the transmit power of D2D users. Using the formula (8a):

$$\frac{p_c H_{c,B}}{p_d H_{d,B} + N_0} \geq r_c^{th} \quad \textbf{(12)}$$

Therefore, the minimum transmit power for a cellular user is:

$$p_c^* = \frac{r_c^{th}}{H_{c,B}} \left(p_d H_{d,B} + N_0 \right) \quad \textbf{(13)}$$

Substitute formula (13) into Shannon's equation to get:

$$R_d = B \log \left[1 + \frac{p_d H_{d,d}}{p_c H_{c,d} + N_0} \right] = B \log \left[1 + \frac{H_{d,d}}{\frac{r_c^{th} H_{d,B} H_{c,d}}{H_{c,B}} + \frac{N_0}{p_d} \left(1 + \frac{r_c^{th} H_{c,d}}{H_{c,B}} \right)} \right] \quad \textbf{(14)}$$

It is clear from the analysis formula (14) that when p_d is raised, the throughput of D2D users will rise as well, with a monotonically rising trend [57]. As a result, to guarantee the cellular users' communication quality, the D2D user d's transmit power should be as high as it can be. It is evident from Figure 2 that:

$$p_d^* = \min \left\{ p_d^{\max}, y_G \right\} \quad \textbf{(15)}$$

Therefore, the optimal transmission power of D2D user d can be obtained from equation (15).

3.3 Multi-stage Matching Algorithm Based on Bipartite Graph

To increase the overall system performance, the D2D resource allocation is turned into a maximum weight matching issue and addressed using a bipartite graph-based multi-stage matching method [58].

3.3.1 Graph Construction

Make a bipartite graph similar to Figure 3 in your mind. It has one edge set and two vertex sets. Vertex set C represents N cellular users, vertex set D represents M D2D couples and the edge set represents a connection. When a cellular user and a D2D pair are connected by edges [59], or when a cellular user and a D2D pair are connected by an edge, the D2D pair is reusing the resource of the cellular user. What defines an edge's weight is the improvement in resource throughput once the cellular user distributes it with the corresponding D2D pair. A subset of the edges in a bipartite graph match each other; no two edges may share the same vertices. Maximum weight matching is the subset of edges whose weight may be maximized [60]. Therefore, finding the best-weighted network that closely resembles Figure 3 will boost throughput. The best weight matching may be achieved using the KM (Kuhn-Munkras) approach.

The KM technique requires that two vertex sets have the same number of vertices [61-62]. A minimum of one virtual vertex must be added if the two sets of vertices are not equal, with the edges between the virtual vertex and other vertices weighting 0.

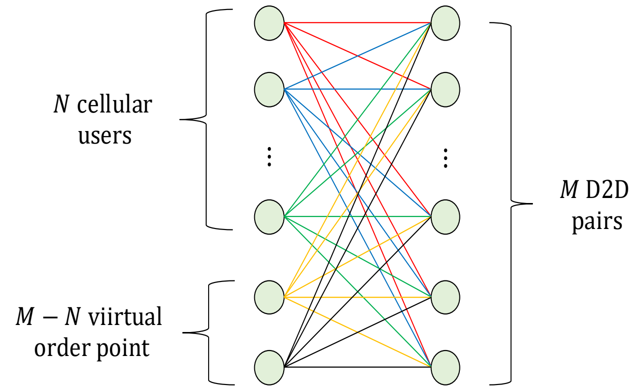

Figure 3. Illustration of a bipartite graph

3.3.2 Algorithm Description

The KM technique may be used to create the bipartite graph afterward to achieve the greatest weight matching in Figure 3. A multi-stage matching approach is utilized to redistribute resources to some D2D pairings because they are assigned to virtual vertices [63-64]. It will be attained at every stage. On the graph, the highest weight match between each pair of phases should be updated. The operation is to update the associated allocation matrix $X = \{x_{c,d}\}_{N \times M}$ [65].

Following the KM algorithm's execution at point G in Figure 2, the matching result shows that N cellular users have been matched with N D2D pairings, resulting in N new vertices, of which C^2 is composed [66]. The unmatched $M-N$ D2D pairs already have a new vertex set, D^2, which includes $d^2(d = 1, 2, \ldots, M-N)$, and at the same time, $M-2N$ virtual vertices join c^2, E^2, which connects c^2 and d^2, and weight W^2, which is the $G^2 = (C^2, D^2, E^3, W^2)$ [67]. The specific phases of the algorithms are shown in Algorithms 1-2.

Algorithm 1. Multi-stage matching

1. Create a bipartite graph for N CUE and M number of D2D pairs
2. If $M \leq N$, add $(N - M)$ to the vertex set of the D2D pair, and then execute the KM algorithm to obtain the distribution result.
3. If $M > N$, add $(M - N)$ to the cellular user vertex set, execute the KM algorithm to get the matching result, then update the bipartite graph, and judge the size of M and N. If $M > N$, repeat this step, Otherwise return to step 2.
4. Until all D2D user pairs are allocated resources. So far, the optimal allocation matrix $X = \{x_{c,d}\}_{N \times M}$ is obtained.

Algorithm 2. KM mechanism

1. Calculate the weight matrix $W_{Z\times Z} = \{w_{x,y}\}_{Z\times Z}$ of the edge set, where, $Z = N$ or $Z = M$, all cellular users $C = \{1, 2, \ldots, N\}$ or all cellular users and the combination of virtual vertices constitutes a vertex set P, and the combination of all D2D users $D = \{1, 2, \ldots, M\}$ and virtual vertices or all D2D users constitutes a vertex set Q, and assigns a top label l_p to each vertex in the set P, where $l_p = \max\{w_{p,1}, w_{p,2}, \ldots, w_{p,2}\}$. Similarly assign a topscript l_q to each vertex in the set Q, where $l_q = 0$, and initialize the matching matrix $M_{Z\times Z}$ to be a zero matrix.
2. From the first vertex in the set P, select the unmatched point with the largest weight value from the set Q to search, and search for the augmenting path. If an unmatched point is passed, it indicates that the search is successful, the path information is updated, the number of matched edges is increased by 1, and the search is no longer performed. If the augmenting path has not been found, the search is stopped from this point.
3. Add this augmenting path in the matching subgraph.
4. If no complete match is found, then the top mark value needs to be modified. The P vertex set on this path is S, and the Q vertex set is T. For all points in S and not in T, calculate the difference $a = \{l_p + l_q - w_{p,q}\}$, from P in the S set subtract a from the top mark, and add a to the Q top mark in the set T .
5. Repeat steps 3 and 4 until finding the complete matching of equal subgraphs with edge weights of all bipartite graphs satisfying $l_p + l_q = w_{p,q}$, that is, finding the matching matrix $M_{Z\times Z}$.

To sum up, the steps of a resource allocation scheme for D2D users proposed in this paper are as follows in Algorithm 3.

Algorithm 3. Resource allocation

1. Assuming that the base station knows the coordinates of users in the cell, it can be seen that the set of cellular users is $C = \{c = 1, 2, 3, \ldots, N\}$, and the set of D2D users is $D = \{d = 1, 2, 3, \ldots, M\}$.
2. Find out the set of potential multiplexed cellular users Π_d for each D2D user. Calculate the intersection point A obtained from formula (9) and judge whether it satisfies the requirements of formula (10). If so, it will be stored in the set Π_d, $x_{c,d} = 1$, otherwise, $x_{c,d} = 0$.
3. According to $p_d^* = \min\{p_d^{\max}, y_G\}$, select the appropriate D2D transmission power.
4. Construct a bipartite graph and calculate the weight, $w_{c,d} = R_{c,d} - R_{c0}$. If cellular user c is not in the potential multiplexing set of D2D user d, its weight is 0.
5. A multi-stage matching algorithm is performed until each D2D user has the resources to communicate. Use the $t = \lceil M / N \rceil$ times KM algorithm to find the optimal matching result $X^* = \{x^*_{c,d}\}_{N\times M^*}$

3.4 Complexity Evaluation

The time complexity of KM is $O(M^3)$, and since the KM method executes $t = \lceil M / N \rceil$ times, the complexity of the multi-stage matching process is $O(t.M^3)$, according to reference [68]. In this study, the suggested method has an acceptable polynomial time complexity of $O(t.M^3)$ where M and N are of the same order of magnitude.

4 Simulation Results

4.1 Parameters

The proposed algorithm is verified in an outdoor urban cellular network scenario in a 28 GHz mmWave 5G cellular network. The path loss value is based on reference [5]. In this paper, a single-cell scenario is considered, and cellular users and D2D users are randomly distributed in this cell, use MATLAB to simulate in this scenario, the main simulation parameters are shown in Table 1.

Table 1. Simulation parameters

Parameter	Value
Cell radius	500 m
Distance of all users to BS	≥ 35m
Number of Cellular Subscribers	20
D2D distance	10 m
RB bandwidth	180 kHz
Maximum transmit power of cellular users	23 dBm
Cellular user SINR threshold r_c^{th}	0
D2D user SINR threshold r_d^{th}	0
D2D user maximum transmit power	10 dBm
Path loss LOS	$\mu = 61.4$, $\alpha = 2$, $\sigma = 5.8$dB
Path loss NLOS	$\mu = 72$, $\alpha = 2.92$, $\sigma = 8.7$dB
Rice channel K parameter	5
Noise power density	-174 dBm/Hz

4.2 Results

The approach suggested in this study is contrasted in the simulation with the heuristic algorithm and random assignment algorithm in [29]. The random allocation algorithm is that the D2D user multiplexes a cellular user resource at random, regardless of other factors, while the heuristic algorithm [29] is that each D2D user selects the cellular user resource that maximizes the total rate for multiplexing under the condition of satisfying the SINR. When the D2D user distance is 10, Figure 4 shows the relationship between the quantity of D2D pairs and the overall system throughput. Figure 4 shows that when the number of D2D users rises, the system's overall throughput rises as well. Because the method suggested in this work chooses the best D2D users for multiplexing for cellular users, its growth rate is higher than that of the reference approach. As a result, the suggested method outperforms previous reference algorithms in terms of performance.

When there are 30 D2D pairs, Figure 5 shows the relationship curve between the overall system throughput and the D2D user distance. Figure 5 illustrates how the system's overall throughput steadily declines as distance increases, and how the rate of decline gets less and smaller until it eventually starts to stabilize. Before distance=30 m, the total system throughput varies significantly as the distance increases, but at distance=30 m, the total system throughput changes gradually as the distance increases. The reason for this is that when the distance is small, the path loss of the link from the D2D transmitter to the receiver is small, resulting in better link quality, which has a significant impact on the system's overall throughput. Conversely, when the distance is large, the path loss is large, producing poor D2D link quality, which has a minor impact on system throughput. Additionally, it is clear from Figure 5 that the suggested method performs notably better than the comparison algorithm.

With 30 D2D users and a distance of 10 m, Figure 6 shows the variation trend of system throughput with D2D transmit power. Figure 6 illustrates how the throughput improves slowly as the D2D transmission power rises. This is because base station interference increases with D2D transmission power. The cellular link has a bigger influence; hence the system throughput growth trend tends to be flat. Therefore, power regulation of the D2D transmission power is required to enhance the system's performance. Figure 6 further demonstrates the suggested algorithm's superiority to competing plans.

The cumulative distribution function (CDF) of the system throughput at 30 D2D users and a 10 m distance is shown in Figure 7. It illustrates how, with the addition of D2D communication, the system's total throughput may be successfully increased by using a fair resource allocation strategy. To pick the most suitable D2D user for resource sharing for cellular users, the suggested algorithm maximizes the incremental value of throughput. As a result, the system may achieve better throughput than previous methods, thus demonstrating the usefulness of the proposed algorithm.

Figure 8 compares the outage probability of the proposed and existing algorithms. As can be seen from Figure 8, the outage probability of the proposed algorithm is better than existing algorithms, which indicates the improved QoS performance of the proposed algorithm.

Figure 9 compares the energy efficiency of the proposed and existing algorithms under different power levels of D2D users. It can be concluded that the energy efficiency of the proposed algorithm is better than existing algorithms for every value of D2D transmit power. This validates the effectiveness of the proposed algorithm and its energy-efficient performance.

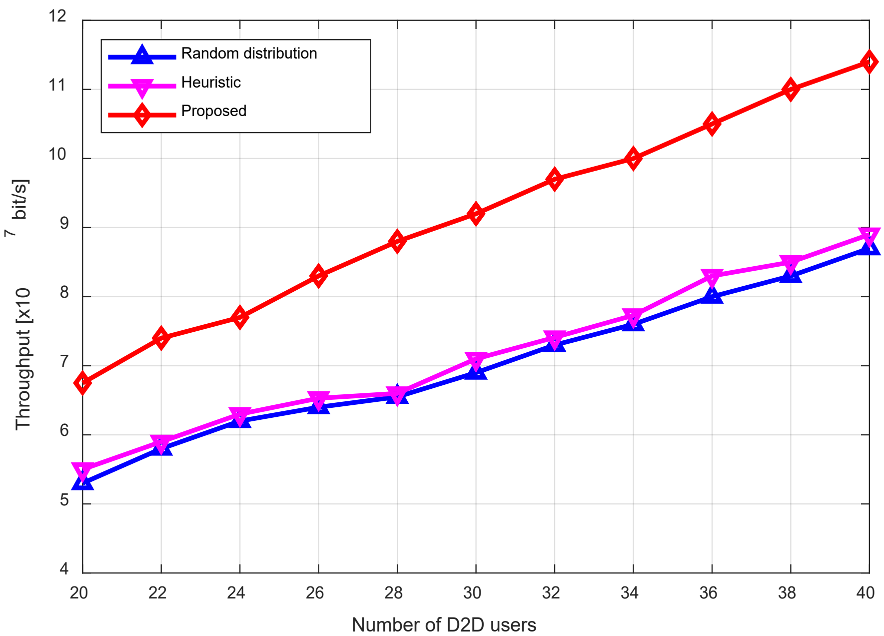

Figure 4. Throughput comparison of the proposed and existing algorithms under an increasing number of D2D users

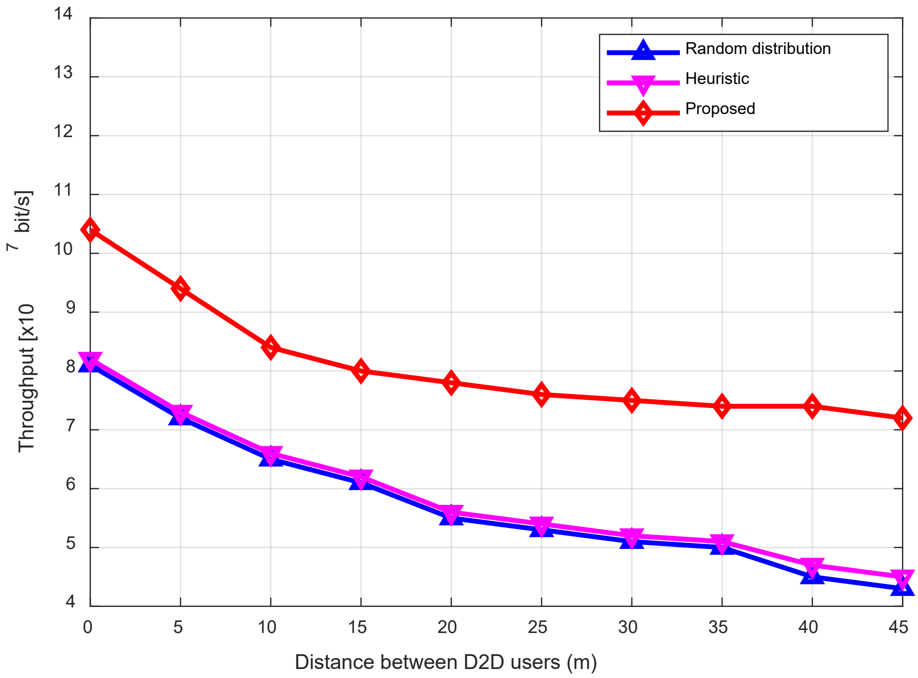

Figure 5. Comparison of throughput of the proposed and existing algorithms under increasing distance

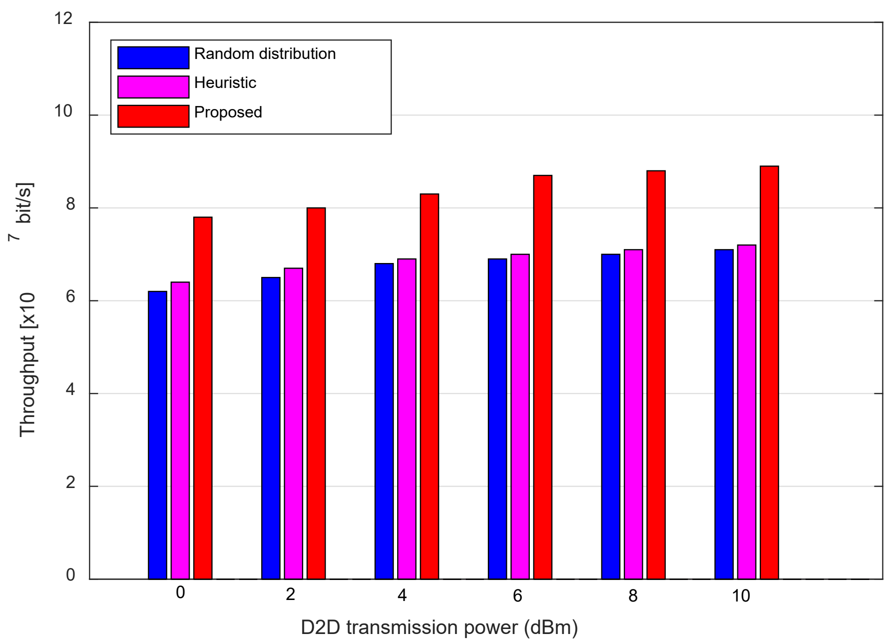

Figure 6. Comparison of throughput of the proposed and existing algorithms under increasing power

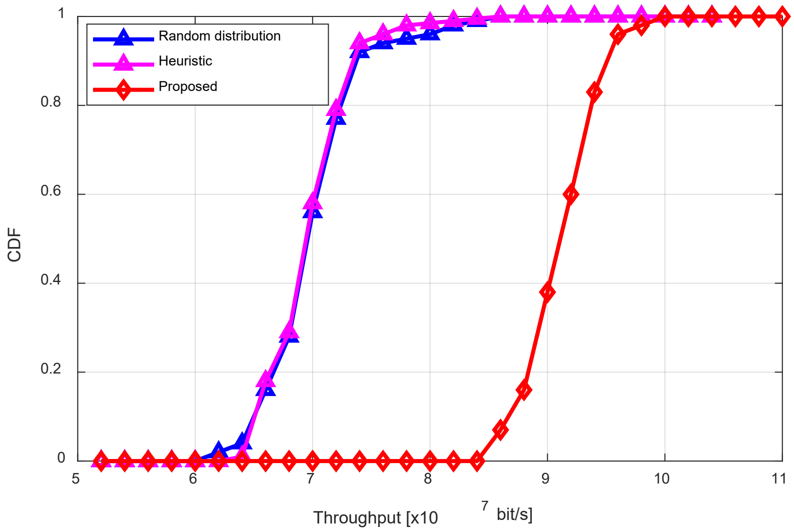

Figure 7. Comparison of CDF of system throughput

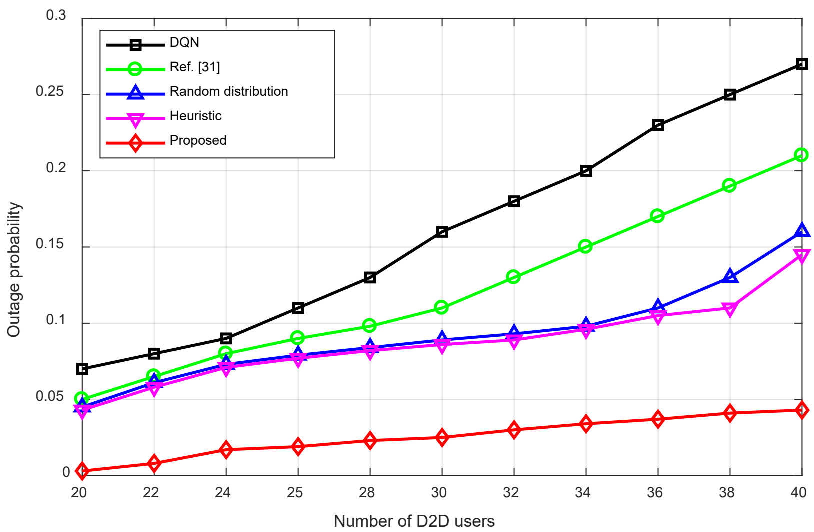

Figure 8. Comparison of outage probability of algorithms

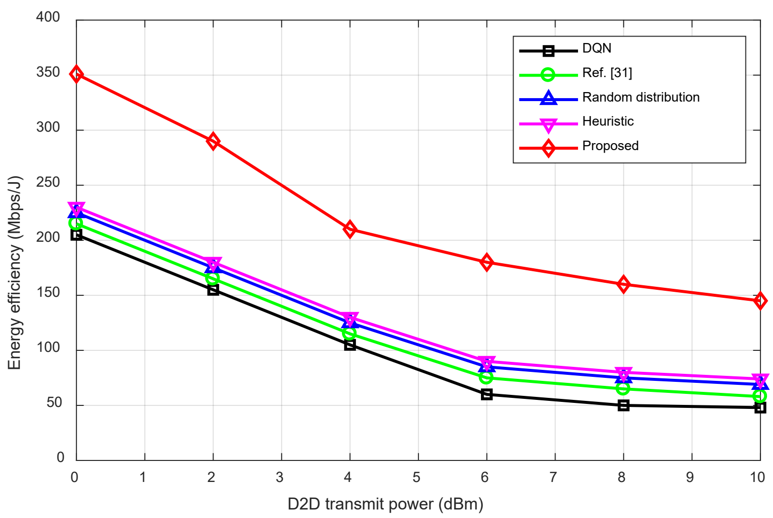

Figure 9. Energy efficiency comparison of algorithms under different transmit power

5 Conclusion

In a 5G network, a single-cell outdoor millimeter-wave scenario is investigated for D2D communication. The system's overall throughput will be maximized by using a resource allocation strategy that is suggested. First, identify the group of cellular users that may be utilized again by D2D users using the linear correlation approach. Second, power control should be applied to D2D users to determine the ideal transmission power. To choose the most appropriate D2D users to share resources with cellular users, a bipartite graph matching technique is developed to distribute resources for D2D users. The simulation results demonstrate that the suggested method may successfully increase system capacity while maintaining the quality of service for D2D and cellular customers.

Further study on multiple cells can be done on the basis that this algorithm does not take the interference of numerous nearby cells into account.

Acknowledgement

This work was financially supported by the Project of Natural Science Foundation of Shandong province (No. ZR2023MF048).

References

[1] Q. Ma, H. Tan, D2D group key agreement scheme for smart devices in HANs, *Journal of Internet Technology*, Vol. 24, No. 3, pp. 659-664, May, 2023.

[2] T. Huynh, T. Onuma, K. Kuroda, M. Hasegawa, W.-J. Hwang, Joint downlink and uplink interference management for device to device communication underlaying cellular networks, *IEEE Access*, Vol. 4, pp. 4420-4430, August, 2016.

[3] B. Gabrovsek, T. Novak, J. Povh, D. R. Poklukar, J. Zerovnik, Multiple Hungarian method for k-assignment problem, *Mathematics*, Vol. 8, No. 11, pp. 1-14, November, 2020.

[4] Y. Zhou, B. Cai, X. Ding, Joint power control and resource allocation for optimizing the D2D user performance of full-duplex D2D underlying cellular networks, *Sensors*, Vol. 23, No. 23, pp. 1-19, December, 2023.

[5] F. Song, Y. Liu, D. Shen, L. Li, J. Tan, Learning control for motion coordination in wafer scanners: toward gain adaptation, *IEEE Transactions on Industrial Electronics*, Vol. 69, No. 12, pp. 13428-13438, December, 2022.

[6] C. Liu, T. Wu, Z. Li, T. Ma, J. Huang, Robust online tensor completion for IoT streaming data recovery, *IEEE Transactions on Neural Networks and Learning Systems*, Vol. 34, No. 12, pp. 10178-10192, December, 2023.

[7] X. Zhou, L. Zhang, SA-FPN: An effective feature pyramid network for crowded human detection, *Applied Intelligence*, Vol. 52, No. 11, pp. 12556-12568, September, 2022.

[8] X. Liang, Z. Huang, S. Yang, L. Qiu, Device-free motion & trajectory detection via RFID, *ACM Transactions on Embedded Computing Systems*, Vol. 17, No. 4, Article No. 78, July, 2018.

[9] C. Zhao, C. Cheung, P. Xu, High-efficiency sub-microscale uncertainty measurement method using pattern recognition, *ISA Transactions*, Vol. 101, pp. 503-514, June, 2020.

[10] K. Xu, Y. Guo, Y. Liu, X. Deng, Q. Chen, Z. Ma, 60-GHz compact dual-mode on-chip bandpass filter using GaAs technology, *IEEE Electron Device Letters*, Vol. 42, No. 8, pp. 1120-1123, August, 2021.

[11] A. Li, C. Masouros, A. Swindlehurst, W. Yu, 1-Bit massive MIMO transmission: embracing interference with symbol-level precoding, *IEEE Communications Magazine*, Vol. 59, No. 5, pp. 121-127, May, 2021.

[12] A. Li, C. Masouros, B. Vucetic, Y. Li, A. Swindlehurst, Interference exploitation precoding for multi-level modulations: closed-form solutions, *IEEE Transactions on Communications*, Vol. 69, No. 1, pp. 291-308, January, 2021.

[13] Y. Deng, J. Lv, D. Huang, S. Du, Combining the theoretical bound and deep adversarial network for machinery open-set diagnosis transfer, *Neurocomputing*, Vol. 548, Article No. 126391, September, 2023.

[14] X. Zhang, S. Wen, L. Yan, J. Feng, Y. Xia, A hybrid-convolution spatial-temporal recurrent network for traffic flow prediction, *The Computer Journal*, Vol. 67, No. 1, pp. 236-252, January 2024.

[15] B. Li, X. Zhou, Z. Ning, X. Guan, K. Yiu, Dynamic event-triggered security control for networked control systems with cyber-attacks: A model predictive control approach, *Information Sciences*, Vol. 612, pp. 384-398, October, 2022.

[16] Y. Zheng, X. Lv, L. Qian, X. Liu, An optimal BP neural network track prediction method based on a GA-ACO hybrid algorithm, *Journal of Marine Science and Engineering*, Vol. 10, No. 10, Article No. 1399, October, 2022.

[17] L. Qian, Y. Zheng, L. Li, Y. Ma, C. Zhou, D. Zhang, A new method of inland water ship trajectory prediction based on long short-term memory network optimized by genetic algorithm, *Applied Sciences*, Vol. 12, No. 8, pp. 1-16, April, 2022.

[18] J. Chen, Q. Wang, W. Peng, H. Xu, X. Li, W. Xu, Disparity-based multiscale fusion network for transportation detection, *IEEE Transactions on Intelligent Transportation Systems*, Vol. 23, No. 10, pp. 18855-18863, October, 2022.

[19] Z. Zhao, G. Xu, N. Zhang, Q. Zhang, Performance analysis of the hybrid satellite-terrestrial relay network with opportunistic scheduling over generalized fading channels, *IEEE Transactions on Vehicular Technology*, Vol. 71, No. 3, pp. 2914-2924, March, 2022.

[20] X. Zhang, S. Fang, Y. Shen, X. Yuan, Z. Lu, Hierarchical velocity optimization for connected automated vehicles with cellular vehicle-to-everything communication at continuous signalized intersections, *IEEE Transactions on Intelligent Transportation Systems*, Vol. 25, No. 3, pp. 2944-2955, March, 2024.

[21] F. Guo, W. Zhou, Q. Lu, C. Zhang, Path extension similarity link prediction method based on matrix algebra in directed networks, *Computer Communications*, Vol. 187, pp. 83-92, April, 2022.

[22] Y. Yao, J. Zhao, Z. Li, X. Cheng, L. Wu, Jamming and eavesdropping defense scheme based on deep reinforcement learning in autonomous vehicle networks, *IEEE Transactions on Information Forensics and Security*, Vol. 18, pp. 1211-1224, January, 2023.

[23] Y. Yao, F. Shu, Z. Li, X. Cheng, L. Wu, Secure transmission scheme based on joint radar and communication in mobile vehicular networks, *IEEE Transactions on Intelligent Transportation Systems*, Vol. 24, No. 9, pp. 10027-10037, September, 2023.

[24] K. Cao, B. Wang, H. Ding, L. Lv, R. Dong, T. Cheng, Improving physical layer security of uplink NOMA via energy harvesting jammers, *IEEE Transactions on Information Forensics and Security*, Vol. 16, pp. 786-799, 2021.

[25] Q. Li, H. Lin, X. Tan, S. Du, H∞ consensus for multiagent-based supply chain systems under switching topology and uncertain demands, *IEEE Transactions on Systems, Man, and Cybernetics: Systems*, Vol. 50, No. 12, pp. 4905-4918, December, 2020.

[26] Y. Chen, Z. Chen, D. Guo, Z. Zhao, T. Lin, C. Zhang, Underground space use of urban built-up areas in the central city of Nanjing: Insight based on a dynamic population distribution, *Underground Space*, Vol. 7, No. 5, pp. 748-766, October, 2022.

[27] X. Li, Y. Sun, Stock intelligent investment strategy based on support vector machine parameter optimization algorithm, *Neural Computing and Applications*, Vol. 32, No. 6, pp. 1765-1775, March, 2020.

[28] Y. Mao, Y. Zhu, Z. Tang, Z. Chen, A novel airspace planning algorithm for cooperative target localization, *Electronics*, Vol. 11, No. 18, pp. 1-18, September, 2022.

[29] S. Li, H. Chen, Y. Chen, Y. Xiong, Z. Song, Hybrid method with parallel-factor theory, a support vector machine, and particle filter optimization for intelligent machinery failure identification, *Machines*, Vol. 11, No. 8, pp. 1-18, August, 2023.

[30] B. Cao, J. Zhao, Y. Gu, S. Fan, P. Yang, Security-aware industrial wireless sensor network deployment optimization, *IEEE Transactions on Industrial Informatics*, Vol. 16, No. 8, pp. 5309-5316, August, 2020.

[31] B. Cao, J. Zhao, Y. Gu, Y. Ling, X. Ma, Applying graph-based differential grouping for multiobjective large-scale optimization, *Swarm and Evolutionary Computation*, Vol. 53, Article No. 100626, March, 2020.

[32] B. Cao, J. Zhao, P. Yang, Y. Gu, K. Muhammad, J. Rodrigues, Multiobjective 3-D topology optimization of next-generation wireless data center network, *IEEE Transactions on Industrial Informatics*, Vol. 16, No. 5, pp. 3597-3605, May, 2020.

[33] B. Cao, S. Fan, J. Zhao, S. Tian, Z. Zheng, Y. Yan, Large-scale many-objective deployment optimization of edge servers, *IEEE Transactions on Intelligent Transportation Systems*, Vol. 22, No. 6, pp. 3841-3849, June, 2021.

[34] B. Cao, J. Zhao, Z. Lv, P. Yang, Diversified personalized recommendation optimization based on mobile data, *IEEE Transactions on Intelligent Transportation Systems*, Vol. 22, No. 4, pp. 2133-2139, April, 2021.

[35] Q. Liu, H. Yuan, R. Hamzaoui, H. Su, J. Hou, H. Yang, Reduced reference perceptual quality model with application to rate control for video-based point cloud compression, *IEEE Transactions on Image Processing*, Vol. 30, No. 1, pp. 6623-6636, July, 2021.

[36] H. Wu, S. Jin, W. Yue, Pricing policy for a dynamic spectrum allocation scheme with batch requests and impatient packets in cognitive radio networks, *Journal of Systems Science and Systems Engineering*, Vol. 31, No. 2, pp. 133-149, April, 2022.

[37] Y. Wang, X. Han, S. Jin, MAP based modeling method and performance study of a task offloading scheme with time-correlated traffic and VM repair in MEC systems, *Wireless Networks*, Vol. 29, No. 1, pp. 47-68, January, 2023.

[38] X. Huang, S. Huang, A. Shui, Government spending and intergenerational income mobility: Evidence from China, *Journal of Economic Behavior & Organization*, Vol. 191, No. 1, pp. 387-414, November, 2021.

[39] Z. Li, X. Zhou, S. Huang, Managing skill certification in online outsourcing platforms: A perspective of buyer-determined reverse auctions, *International Journal of Production Economics*, Vol. 238, Article No. 108166, August, 2021.

[40] J. Luo, Y. Wang, G. Li, The innovation effect of administrative hierarchy on intercity connection: The machine learning of twin cities, *Journal of Innovation & Knowledge*, Vol. 8, No. 1, pp. 1-16, January-March, 2023.

[41] J. Luo, G. Wang, G. Li, G. Pesce, Transport infrastructure connectivity and conflict resolution: a machine learning analysis, *Neural Computing and Applications*, Vol. 34, No. 9, pp. 6585-6601, May, 2022.

[42] H. Jiang, X. Dai, Z. Xiao, A. Iyengar, Joint task offloading and resource allocation for energy-constrained mobile edge computing, *IEEE Transactions on Mobile Computing*, Vol. 22, No. 7, pp. 4000-4015, July, 2023.

[43] H. Jiang, M. Wang, P. Zhao, Z. Xiao, S. Dustdar, A utility-aware general framework with quantifiable privacy preservation for destination prediction in LBSs, *IEEE/ACM Transactions on Networking*, Vol. 29, No. 5, pp. 2228-2241, October, 2021.

[44] X. Xiao, H. Fang, H. Jiang, J. Bai, V. Havyarimana, H. Chen, Understanding private car aggregation effect via spatio-temporal analysis of trajectory data, *IEEE Transactions on Cybernetics*, Vol. 53, No. 4, pp. 2346-2357, April, 2023.

[45] Y. Chen, Research on collaborative innovation of key common technologies in new energy vehicle industry based on digital twin technology, *Energy Reports*, Vol. 8, pp. 15399-15407, November, 2022.

[46] B. Chen, J. Hu, Y. Zhao, B. Ghosh, Finite-time velocity-free rendezvous control of multiple AUV systems with intermittent communication, *IEEE Transactions on Systems, Man, and Cybernetics: Systems*, Vol. 52, No.

10, pp. 6618-6629, October, 2022.

[47] Y. Peng, Y. Zhao, J. Hu, On the role of community structure in evolution of opinion formation: A new bounded confidence opinion dynamic, *Information Sciences*, Vol. 621, pp. 672-690, April, 2023.

[48] Y. Jiang, X. Li, Broadband cancellation method in an adaptive co-site interference cancellation system, *International Journal of Electronics*, Vol. 109, No. 5, pp. 854-874, 2022.

[49] Y. Jiang, S. Liu, M. Li, N. Zhao, M. Wu, A new adaptive co-site broadband interference cancellation method with auxiliary channel, *Digital Communications and Networks*, Vol. 10, No. 4, pp. 934-947, August, 2024.

[50] G. Chen, P. Chen, W. Huang, J. Zhai, Continuance intention mechanism of middle school student users on online learning platform based on qualitative comparative analysis method, *Mathematical Problems in Engineering*, Vol. 2022, No. 1, pp. 1-12, March, 2022.

[51] Q. Liao, H. Chai, H. Han, X. Zhang, X. Wang, W. Xia, An integrated multi-task model for fake news detection, *IEEE Transactions on Knowledge and Data Engineering*, Vol. 34, No. 11, pp. 5154-5165, November, 2022.

[52] S. Jiang, C. Zhao, Y. Zhu, C. Wang, Y. Du, A practical and economical ultra-wideband base station placement approach for indoor autonomous driving systems, *Journal of Advanced Transportation*, Vol. 22, No. 2, pp. 1-12, March, 2022.

[53] Q. Ni, J. Guo, W. Wu, H. Wang, Influence-based community partition with sandwich method for social networks, *IEEE Transactions on Computational Social Systems*, Vol. 10, No. 2, pp. 819-830, April 2023.

[54] Q. Ni, J. Guo, W. Wu, H. Wang, J. Wu, Continuous influence-based community partition for social networks, *IEEE Transactions on Network Science and Engineering*, Vol. 9, No. 3, pp. 1187-1197, May-June, 2022.

[55] G. Zhou, R. Zhang, S. Huang, Generalized buffering algorithm, *IEEE access*, Vol. 9, No. 1, pp. 27140-27157, February, 2021.

[56] Q. She, R. Hu, J. Xu, M. Liu, K. Xu, H. Huang, Learning high-DOF reaching-and-grasping via dynamic representation of gripper-object interaction, *ACM Transactions on Graphics*, Vol. 41, No. 4, pp. 1-14, July, 2022.

[57] H. Yuan, B. Yang, System dynamics approach for evaluating the interconnection performance of cross-border transport infrastructure, *Journal of Management in Engineering*, Vol. 38, No. 3, pp. 1-13, May, 2022.

[58] J. Zhang, Y. Liu, Z. Li, Y. Lu, Forecast-assisted service function chain dynamic deployment for SDN/NFV-enabled cloud management systems, *IEEE Systems Journal*, Vol. 17, No. 3, pp. 4371-4382, September, 2023.

[59] K. Zhao, Z. Jia, F. Jia, H. Shao, Multi-scale integrated deep self-attention network for predicting remaining useful life of aero-engine, *Engineering Applications of Artificial Intelligence*, Vol. 120, Article No. 105860, April, 2023.

[60] J. Shi, W. Niu, Z. Li, C. Shen, J. Zhang, S. Yu, Optimal adaptive waveform design utilizing an end-to-end learning-based pre-equalization neural network in an UVLC system, *Journal of Lightwave Technology*, Vol. 41, No. 6, pp. 1626-1636, March, 2023.

[61] J. Shi, Z. Li, J. Jia, Z. Li, C. Shen, J. Zhang, Waveform-to-waveform end-to-end learning framework in a seamless fiber-terahertz integrated communication system, *Journal of Lightwave Technology*, Vol. 41, No. 8, pp. 2381-2392, April, 2023.

[62] D. Zhou, M. Sheng, J. Li, Z. Han, Aerospace integrated networks innovation for empowering 6G: A survey and future challenges, *IEEE Communications Surveys & Tutorials*, Vol. 25, No. 2, pp. 975-1019, Secondquarter, 2023.

[63] J. Tan, H. Jin, H. Hu, R. Hu, H. Zhang, H. Zhang, WF-MTD: Evolutionary decision method for moving target defense based on wright-fisher process, *IEEE Transactions on Dependable and Secure Computing*, Vol. 20, No. 6, pp. 4719-4732, November-December, 2023.

[64] B. Cheng, M. Wang, S. Zhao, Z. Zhai, D. Zhu, J. Chen, Situation-aware dynamic service coordination in an IoT environment, *IEEE/ACM Transactions on Networking*, Vol. 25, No. 4, pp. 2082-2095, August, 2017.

[65] S. Lu, Y. Ding, M. Liu, Z. Yin, L. Yin, W. Zheng, Multiscale feature extraction and fusion of image and text in VQA, *International Journal of Computational Intelligence Systems*, Vol. 16, No. 1, pp. 1-11, April, 2023.

[66] S. Lu, M. Liu, L. Yin, Z. Yin, X. Liu, Z. Zheng, The multi-modal fusion in visual question answering: a review of attention mechanisms, *PeerJ Computer Science*, Vol. 9, No. 1, pp. 1-29, May, 2023.

[67] X. Liu, T. Shi, G. Zhou, M. Liu, Z. Yin, L. Yin, W. Zheng, Emotion classification for short texts: an improved multi-label method, *Humanities and Social Sciences Communications*, Vol. 10, No. 1, pp. 1-9, June, 2023.

[68] X. Liu, S. Wang, S. Lu, Z. Yin, X. Li, L. Yin, J. Tian, W. Zheng, Adapting feature selection algorithms for the classification of chinese Texts, *Systems*, Vol. 11, No. 9, Article No. 483, September, 2023.

Biographies

Dong Sang received the Bachelor's and Master's degrees in Engineering from the School of Physics & Electronic Science, Shandong Normal University, Jinan, China, in 2010 and 2014, respectively. He is currently an assistant with the School of computer science, Weifang University of Science and Technology, Weifang 262700, China. His current research interests are process mining, sensor networks and machine learning.

Hongwei Sun received the B.S. and M.S. degrees from the school of Engineering, Qufu Normal University, Rizhao, China, in 2013 and 2016, respectively, and the Ph.D. degree in computer software and theory from Shandong University of Science and Technology, Qingdao, China, in 2022. He is currently an associate professor with the College of Mathematics and Applied Computer Technology, Jining University, Qufu 273155, China. His current research interests are process mining, Petri nets, sensor networks, machine learning, and workflow.